Struct Chem (2015) 26:1585–1601
DOI 10.1007/s11224-015-0682-9

ORIGINAL RESEARCH

Encapsulation of monomers, homodimers and heterodimers of amides and carboxylic acids in three non-covalent assemblies

Demeter Tzeli[1] · Ioannis D. Petsalakis[1] · Giannoula Theodorakopoulos[1] · Julius Rebek Jr.[2,3]

Received: 12 August 2015 / Accepted: 14 September 2015 / Published online: 7 October 2015

Abstract A structural study has been carried out involving geometry optimization of different capsules and encapsulated complexes of single monomers, homodimers and heterodimers of benzoic acid and benzamide and substituted dimers, as well as hydrogen-bonded networks of benzamide addressing experimental observation, where cages offering similar cavities but made up of slightly different cavitands result in strikingly different dimer distributions. This is attributed, according to the present results, mainly to the fact that the two cages have different formation energy and different dimer encapsulation energy. The generation of hydrogen-bonded networks of the amide in solution acts competitively to encapsulation. In addition, the trends of the different quantities associated with encapsulation such as dimerization energy, % dimer distribution and encapsulation energies, as the size of the dimers is increased, are examined. Furthermore, the efficacy of the ONIOM(DFT or MP2 and CCSD:PM6) method with respect to the calculation of % distribution of encapsulated dimers in limited cavities is studied. The results show that when the interaction of the guests with the cage is significant, the ONIOM % distributions do not agree with the experimental finding, as full DFT does, due to PM6 method, where the use of semi-empirical PM6 method changes the ordering of the low in energy encapsulated complexes.

Keywords Encapsulation · Hydrogen bonding · Dimers · Carboxylic acid · Amide · Benzoic acid · Benzamide · Hydrogen-bonded network · DFT calculations

Introduction

Molecular containers holding one or more guest species inside are of great interest for molecular recognition [1–3]. Moreover, the interior of a cavity can stabilize reactive species by isolating guests from the bulk environment and can accelerate reactions effectively due to guest discrimination. As a result, the scope of cages and capsules that have been studied to date is widespread with cavities of differing sizes and shapes. Containers can be made as single, large covalently joined molecules [4, 5], or the capsules can also be achieved via non-covalent assemblies of molecules which can assemble in solution around the guests [6–11].

In solution, non-covalent assemblies exist in equilibrium between the capsule and the individual parts. The entry and the exit of guests can take place as the capsule is continually assembling and disassembling, with the guest exchange limited by the rate at which the dissociation of the capsule occurs. The guests in such species can be fully

This paper is dedicated to Professor Magdolna Hargittai on the occasion of her 70th birthday.

Electronic supplementary material The online version of this article (doi:10.1007/s11224-015-0682-9) contains supplementary material, which is available to authorized users.

✉ Demeter Tzeli
dtzeli@eie.gr

✉ Ioannis D. Petsalakis
idpet@eie.gr

[1] Theoretical and Physical Chemistry Institute, National Hellenic Research Foundation, 48 Vassileos Constantinou Ave., 116 35 Athens, Greece

[2] Skaggs Institute for Chemical Biology, Department of Chemistry, The Scripps Research Institute, 10550 North Torrey Pines Road, La Jolla, CA 92037, USA

[3] Department of Chemistry, Fudan University, 220 Handan Road, Shanghai 20433, China

enclosed with no contact with the external environment. The variety of non-covalent capsules can be readily divided into those which are assembled from several different species and those which are composed of two or more self-complimentary molecules [6–12].

One of the interactions most commonly utilized by nature and by the supramolecular synthetic organic chemists is the hydrogen bond [8]. The directionality and relative selectivity offered by this interaction make it very appealing in most cases. Capsules created by hydrogen bonding have the potential to act as excellent host species and the large amount of current research in this area can be seen in recent reviews [7, 9]. Hydrogen bonding is one of the most studied methods of forming non-covalent capsules, while other interactions such as electrostatic interactions [13, 14] and metal/ligand interactions [15, 16] are also used in the design of molecular capsules.

The nature and the strength of hydrogen bond have been studied both experimentally (mainly in small molecules) and theoretically for many systems [17–22]. Note that the observation of individual hydrogen-bonded dimers in solution is difficult because of their short lifetimes and the rapid exchange of partners; however, reversible encapsulation allows the temporary isolation of the guest dimers by mechanical barriers and their characterization by NMR methods at normal conditions [23–25].

Recently, theoretical research has been carried out on the relative stability of encapsulated homodimers and heterodimers of amides, boronic acids and carboxylic acids in capsules with sufficiently large cavities for the dimers [26], in capsules with confined cavities [27], and tight or very limited cavity [28, 29]. Corresponding experimental data [23, 25] show that experiment and theory determine the % distributions of the encapsulated dimers in good agreement [26, 27]. Furthermore, it was shown that the size of the cage affects the % distribution: When the capsule is large enough to accommodate the dimers without any significant compression, the dimerization energy ordering of the different encapsulated dimers has been found to be practically the same as that in the gas phase [26, 27]. In smaller cages where the dimers still fit well in the cage, hydrogen bonding interactions of the amide segments with the cage are formed and the hydrogen bonds in the corresponding dimers are weakened resulting in lower dimerization energy and different % distribution from those in the larger cage and the free dimers [25, 27]. On the contrary, in very limited cavities while encapsulation is still favorable, dimerization does not occur and the result is two co-encapsulated monomers. This is in accord with the fact that for the last case of very tight cages, encapsulated dimers have not been found experimentally [29].

While as shown above a great deal of theoretical work has been carried out on different aspects of encapsulated complexes, further work is required in order to address further experimental observations: For example, it may be noted that in cages offering similar cavities but made up of slightly different cavitands result in strikingly different encapsulated dimer distribution, as will be described below [25]. In the present work, a structural study involving geometry optimization of different capsules and encapsulated complexes as well as hydrogen-bonded network of amide is presented, addressing the above observation. It is also of interest to examine the trends of the different quantities associated with encapsulation such as dimerization energy, % dimer distribution, encapsulation energies and formation energies of the complexes, as the size of the dimers is increased. Furthermore, of theoretical interest is to determine the efficacy of the ONIOM(DFT or MP2 and CCSD:PM6) with respect to the calculation of % distribution of encapsulated dimers in limited cavities; we already know that for capsules with sufficiently large cavities for the dimers, the ONIOM(DFT:PM6) present the same % distribution with full DFT methods [26]. This latter consideration is of significance since the size of the systems under study is quite large, while determination of the true minimum energy geometry by geometry optimization is very difficult as the interactions are generally weak and slight geometry alterations are energetically easy. Accordingly, the use of the ONIOM(DFT:PM6) method for cases where its reliability is established presents a great saving in computational effort.

Computational details

DFT (M06-2X [30, 31] and ωB97X-D [32]), MP2 and CCSD calculations were carried out in conjunction with the 6-31G(d,p), 6-311 + G(d,p) and 6-311 ++ G(d,p) basis sets [33]. All calculated structures are fully optimized. Moreover, the fast ONIOM(M06-2X or MP2 or CCSD:PM6) methodology [34–36], where the systems were defined as two regions (layers), has been employed. The high layer consists of the guests calculated at the M06-2X/6-31G(d,p), M06-2X/6-311 + G(d,p) level, MP2/6-31G(d,p) and CCSD/6-31G(d,p) levels of theory, and the low layer is the capsule calculated at the PM6 level of theory. Note that the calculated here encapsulated complexes are large, having 230–308 atoms and the cages have 200–264 atoms.

Previous studies have shown that the use of M06-2X and ωB97X-D functionals for the calculation of the free and encapsulated dimers leads to satisfactory results, as compared to experimental data [29, 37]. Moreover, the effect of inclusion of diffuse functions was found to be not significant for the encapsulated dimers considering the great increase in computational effort involved [28]. Finally, the ONIOM(DFT:PM6) method has been found adequate for the calculations of the encapsulated structures in a cage with a large cavity [26].

The three cages employed in the present work, **1.1**, **1.2$_4$.1** and **3.3,** are depicted in Fig. 1. Cages **1.1** and **3.3** consist of two cavitands **1** and two cavitands **3,** respectively [38, 39], while cage **1.2$_4$.1** consists of two cavitands **1** and four spacers **4** [23], see Fig. 1. The heterodimers and homodimers of benzoic acid (**C$_H$**), p-methylbenzoic acid (**C$_M$**), p-ethylbenzoic acid (**C$_E$**), benzamide (**A$_H$**) p-methylbenzamide (**A$_M$**) and p-ethyl benzamide (**A$_E$**) are shown in Fig. 2. The encapsulated monomers and dimers are shown in Figs. 3, 4, 5. The encapsulated complexes are named here with the name of the capsule followed by the abbreviation of the dimer and a number that shows the relative ordering of the isomer, for example, **3.3_AA$_H$-1** stands for the lowest minimum structure (1) of encapsulated benzamide homodimer (**AA$_H$**) in the **3.3** cage. Finally, in order to study the tendency of amide to form hydrogen networks, clusters of three, four, five and six benzamide molecules were also calculated here.

All encapsulation, formation and dimerization energies presented here have been corrected with respect to the basis set superposition error (BSSE) via the counterpoise procedure [40, 41]. The theoretical % distribution of the different dimers has been introduced previously [26, 37], based on the BSSE-corrected dimerization energy and statistical factors, i.e., the occurrence of the heterodimers is twice as probable as the homodimers, see Electronic Supporting materials (ESM) for detailed description. All calculations were carried out using the Gaussian 09 program [42].

The particulars of the calculations will be described in the following sections along with the results, where use is

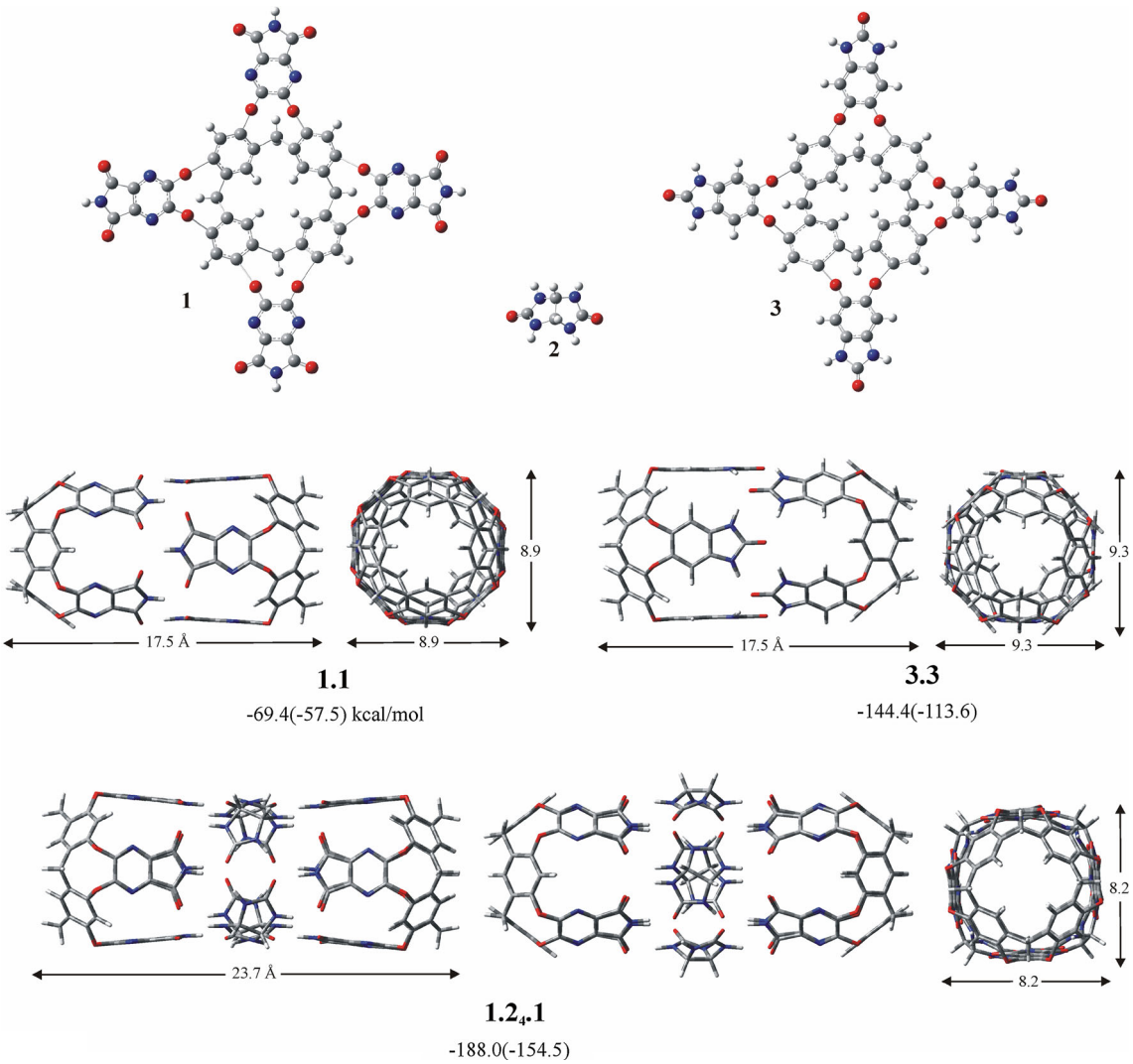

Fig. 1 Cavitands **1** and **3**, spacer **2** and capsules **1.1**, **3.3** and **1.2$_4$.1** viewed from two different angles, i.e., along the central axis of the capsule and end-on view (Color online; H atoms = *white spheres*, C = *gray spheres*, O = *red spheres* and N = *blue spheres*). Geometry and formation energy of the cage with respect to the free cavitands (and spacers) fixed in the geometry of the capsule (to the free optimized cavitands) at the M06-2X/6-31G(d,p) level of theory

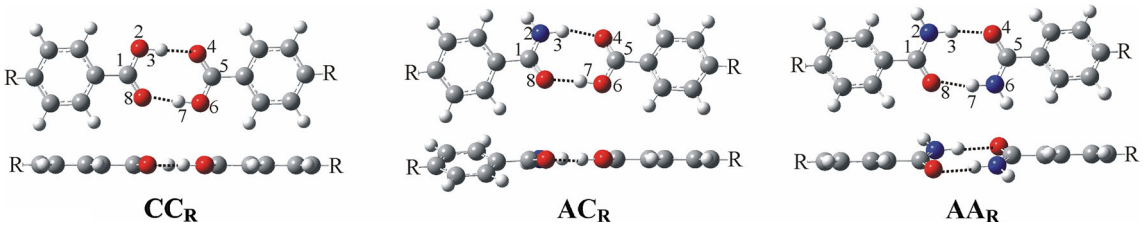

Fig. 2 Homodimers and heterodimers of amide ($\mathbf{A_R}$) and carboxylic acid ($\mathbf{C_R}$) with R = H, methyl and ethyl group (Color online; H atoms = *white spheres*, C = *gray spheres*, O = *red spheres* and N = *blue spheres*)

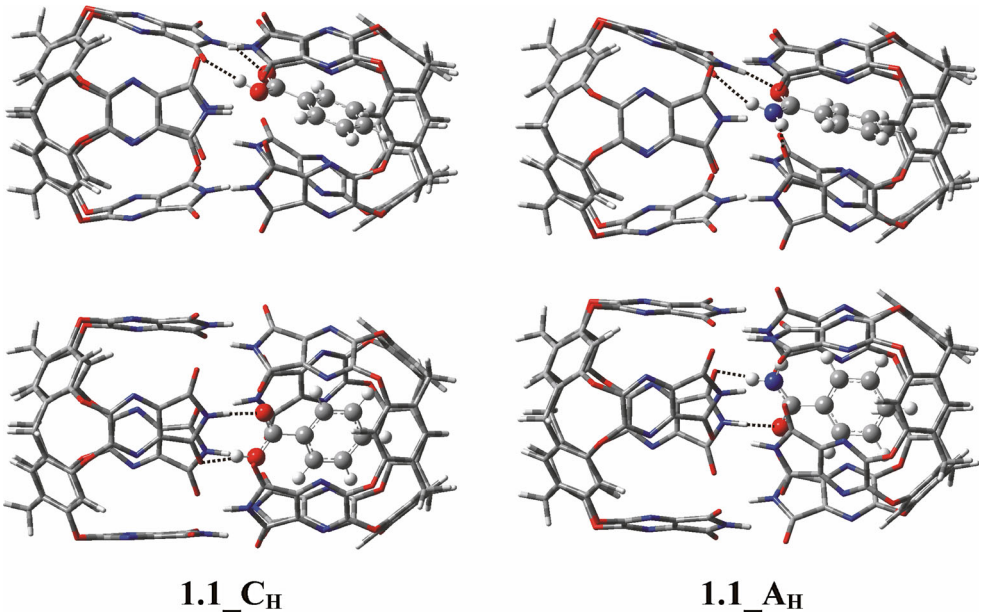

Fig. 3 Calculated structures of the lowest minima of the **1.1_A$_H$** and **1.1_C$_H$** species viewed from two different angles (Color online; H atoms = *white spheres*, C = *gray spheres*, O = *red spheres* and N = *blue spheres*). The atoms of the capsule are designated with stick bonds for clarity

also made of our previous calculations and available experimental data, as appropriate.

Results and discussion

Free dimers

The free heterodimers and homodimers of the benzamide, benzoic acid and their p-methyl and p-ethyl-substituted species, are depicted in Fig. 2, while some geometrical quantities are listed in Table 1. The structures of the dimers were optimized via DFT methodology using the M06-2X and ωB97X-D functionals, and via the MP2 method in conjunction with the 6-31G(d,p), 6-311 + G(d,p) and 6-311 ++ G(d,p) basis sets. Additional calculations via the CCSD/6-31G(d,p) methodology at the optimized MP2/6-31G(d,p) geometry are carried out. All theoretical levels predict nearly the same geometries. Differences are observed only for the hydrogen bonds. For the OH…O hydrogen bonds, the M06-2X/6-31G(d,p) predicts the shortest lengths. The MP2 methods or the addition of the diffuse functions predicts a significant elongation of the bonds compared to M06-2X/6-31G(d,p) method. However, the best agreement of the theoretical hydrogen bond lengths with the experimental ones are observed for the ωB97X-D/6-31G(d,p) method in the case of **CC$_H$** and **CC$_M$** dimers, see Table 1. For the NH…O hydrogen bonds, all methods predict rather similar values. The largest difference between the methods is 0.06 Å. Finally, we should note the % dimer distribution of the free homodimers and heterodimers is independent of the level of theory. All methods and basis sets predict the same % dimer distribution of the free homodimers and heterodimers, i.e., 27 % for the acid homodimers, 51 % for the heterodimers and 22 % for the amide homodimers.

Encapsulated monomers

The encapsulated single benzoic acid ($\mathbf{C_H}$) and benzamide ($\mathbf{A_H}$) monomers in the **1.1** cage are shown in Fig. 3. The M06-2X/6-31G(d,p) and ωB97X-D/6-31G(d,p) methodology was employed in these calculations. In the lowest energy minimum structures, the guests are placed inside of

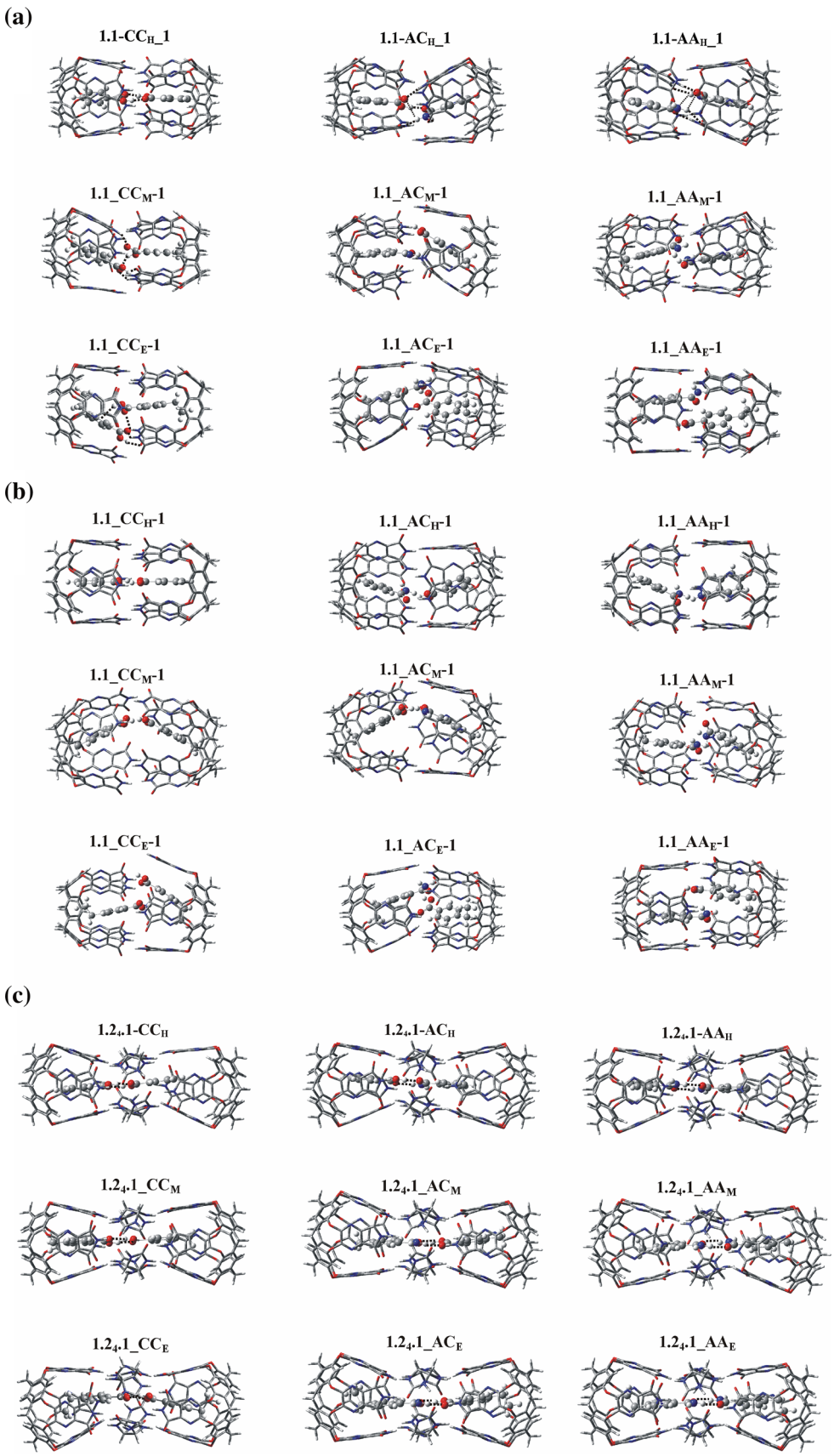

Fig. 4 Calculated structures of the lowest minima of the **1.1_CC$_R$**, **1.1_AA$_R$**, **1.1_AC**, **1.2$_4$.1_CC$_R$**, **1.2$_4$.1_AA$_R$** and **1.2$_4$.1_AC** species. **a** In M06-2X/6-31G(d,p) [similar structures are obtained via ωB97X-D/6-31G(d,p)], **b** in ONIOM(MP2/6-31G(d,p):PM6) [similar structures are obtained via ONIOM(M06-2X or CCSD/6-31G(d,p)] and **c** in M06-2X/6-31G(d,p) methodology [similar structures are obtained via ONIOM(M06-2X or MP2/6-31G(d,p)] (Color online; H atoms = *white spheres*, C = *gray spheres*, O = *red spheres* and N = *blue spheres*)

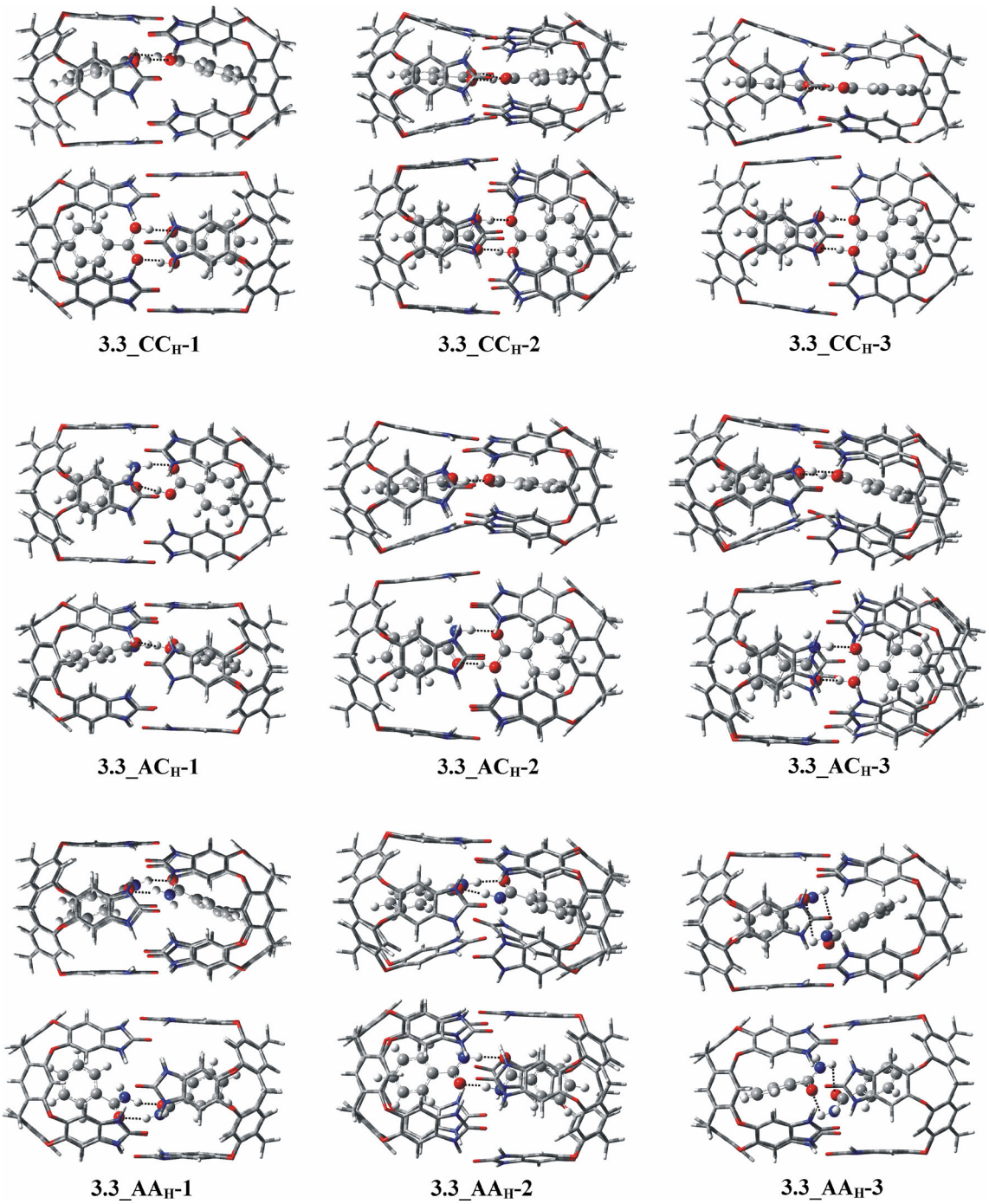

Fig. 5 Calculated structures of the lowest minima of the **3.3_CC**, **3.3_AA** and **3.3_AC** species viewed from two different angles (Color online; H atoms = *white spheres*, C = *gray spheres*, O = *red spheres* and N = *blue spheres*). The atoms of the capsule are designated with stick bonds for clarity

the one cavitand and form two hydrogen bonds with the other cavitand, see Fig. 3 and Table 2. As a result the cage is slightly deformed compared to the free **1.1** cage, see Fig. 1. In addition, the second hydrogen of the amide group of benzamide forms a hydrogen bond with the cavitand where it is placed. The encapsulation energies of the monomers are −14.2 (for $\mathbf{C_H}$) and −17.2 kcal/mol (for $\mathbf{A_H}$) at the M06-2X/6-31G(d,p) level of theory, see Table 1. At the ωB97X-D/6-31G(d,p) level of theory, the values are increased due to the fact that the ωB97X-D functional includes long range and empirical dispersion corrections in calculation of interactions between the guests and the cavitands, see Table 2. We should point out that many weak long-range interactions exist between the

Table 1 Dimerization energies, ΔE (kcal/mol), hydrogen bond distances, R(Å) and % dimer distribution of the free **CC**, **AC** and **AA** species

Methods	ΔE^a **CC_H**	$R_{OH\cdots O}$	%[a]	ΔE^a **AC_H**	$R_{OH\cdots O}$	$R_{NH\cdots O}$	%[a]	ΔE^a **AA_H**	$R_{NH\cdots O}$	%[a]
M06-2X/6-31G(d,p)[b]	−17.8	1.558	27.7	−16.3	1.578	1.844	50.7	−13.9	1.855	21.6
M06-2X/6-311 + G(d,p)[b]	−17.1	1.658	27.2	−16.0	1.633	1.882	50.9	−13.8	1.868	21.9
M06-2X/6-311 ++ G(d,p)	−17.1	1.658	27.2	−16.0	1.633	1.882	50.8	−13.8	1.868	21.9
ωB97X-D/6-31G(d,p)	−18.5	1.628	27.3	−17.1	1.624	1.830	50.6	−14.9	1.829	22.1
ωB97X-D/6-311 + G(d,p)	−17.7	1.661	26.9	−16.7	1.644	1.858	50.7	−14.7	1.840	22.4
MP2/6-31G(d,p)	−14.0	1.678	26.8	−13.3	1.666	1.883	50.8	−11.8	1.878	22.4
MP2/6-311 + G(d,p)[b]	−12.9	1.671	26.3	−12.5	1.661	1.888	50.9	−11.2	1.872	22.7
MP2/6-311 ++ G(d,p)	−13.0	1.673	26.3	−12.6	1.662	1.890	51.0	−11.2	1.873	22.7
CCSD/6-31G(d,p)[c]	−13.4	1.678	27.0	−12.6	1.666	1.883	50.8	−11.0	1.878	22.1
Expt[d]		1.635								
	CC_M			**AC_M**				**AA_M**		
M06-2X/6-31G(d,p)[e]	−17.9	1.557	27.8	−16.3	1.582	1.842	50.7	−13.9	1.855	21.6
ωB97X-D/6-31G(d,p)[e]	−18.6	1.627	27.4	−17.1	1.625	1.827	50.6	−14.9	1.829	22.0
Expt[d]		1.636[e]								
	CC_E			**AC_E**				**AA_E**		
M06-2X/6-31G(d,p)[b]	−17.8	1.557	27.7	−16.3	1.582	1.841	50.7	−13.9	1.858	21.6
M06-2X/6-311 + G(d,p)[b]	−17.2	1.657	27.3	−16.0	1.632	1.881	50.9	−13.7	1.867	21.8
ωB97X-D/6-31G(d,p)[e]	−18.5	1.627	27.4	−17.1	1.624	1.829	50.6	−14.9	1.829	22.0

[a] BSSE-corrected dimerization energies

[b] Ref [37]

[c] At the optimized MP2/6-31G(d,p) geometry

[d] Experimental data, Ref. [24]; in CDF_3/CDF_2Cl solution 130 (**CC**) and 120 (**CC_M**) K

[e] Ref. [29]

Table 2 Hydrogen bond distances R(Å) between monomers and cage and encapsulation energy[a] of monomers (ΔE_2 in kcal/mol), and formation energy of the encapsulated complexes with respect to the three components of fully disassembled complexes (ΔE_3 in kcal/mol) of the **1.1_C** and **1.1_A** encapsulated complexes at the M06-2X (first entry) and ωB97X-D(second entry)/6-31G(d,p) levels of theory

Species	$R_{H\ldots O}$	$R_{O\ldots Hc}$	$R^b_{H\ldots Oc}$	ΔE^c_2	ΔE^d_3
1.1_C	1.851	1.965		−14.3	−84.9 (−73.0)
	1.802	1.763		−30.1	−98.7 (−89.1)
1.1_A	2.080	1.777	2.093	−17.2	−88.1 (−76.2)
	2.012	1.690	2.046	−34.1	−103.5 (−93.9)

[a] BSSE-corrected values

[b] The hydrogen bond distance between second hydrogen atom of the amide group and oxygen atom of the cage

[c] $\Delta E_2 = -[E(\text{encapsulated complexes}) - E(\text{cage}) - E(\text{monomer})]$

[d] $\Delta E_3 = -[E(\text{encapsulated complexes}) - 2\ E(\mathbf{1}) - \text{E(monomer)}]$; ΔE_3 energy with respect to the cavitands and spacers in the geometry of the capsule and in parenthesis with respect to the free geometry optimized cavitands and spacers

guests and the cavitands which affect the calculation of the ΔE_1, ΔE_2, ΔE_3 energies. Note that, in the case of the p-methyl- and p-ethyl-substituted dimers encapsulated in the **1.1** cage [29], where the dimers are compressed and do not exist as dimers but as two monomers, encapsulation energies of the monomers correspond to the sum of the corresponding ΔE_2 values of the unsubstituted monomers for both M06-2X and the ωB97X-D methods, since the p-methyl- and p-ethyl-substituted encapsulated monomers and the single encapsulated monomers present the same hydrogen bond interactions with the cage. On the contrary, in the case of the unsubstituted dimers, the ΔE_2 energies are larger than the sum of the corresponding ΔE_2 values of the unsubstituted monomers, see Tables 2 and 3. The corresponding hydrogen bond distances between the monomers and the cage range from 1.54 to 2.06 (**1.1_AA_M** and **1.1_AA_E**) and from 1.70 to 1.89 Å (**1.1_CC_M** and **1.1_CC_E**) [29] similar to the corresponding values of the isolated **C_H** and **A_H** monomers in the **1.1** cage, see Table 2.

Encapsulated dimers in 1.1 and $1.2_4.1$ cages

The encapsulation of the heterodimer **AC_R** and the homodimers **AA_R** and **CC_R** in **1.1** (for R = H) and **$1.2_4.1$** (for R = E, i.e., p-ethyl-substituted benzoic acid/

Table 3 Hydrogen bond distances (R in Å), dimerization energies of the encapsulated $\mathbf{A_H}$ and $\mathbf{C_H}$ guests inside the cage (ΔE, in kcal/mol)[a], encapsulation energy of the dimers (ΔE_1 in kcal/mol)[a], encapsulation energy of the monomers (ΔE_2 in kcal/mol)[a] and formation energy of the encapsulated complexes with respect to the four components of fully disassembled complexes (ΔE_3 in kcal/mol)[a,b] at various levels of theory

	Methods	R_{3-4}	R_{7-8}	ΔE	ΔE_1	ΔE_2	ΔE_3^b
1.1_CC$_H$-1	ONIOM(M06-2X/6-31G(d,p):PM6)	1.532	1.537	−17.7			
	ONIOM(M06-2X/6-311 + G(d,p):PM6)	1.640	1.657	−16.2			
	ONIOM(MP2/6-31G(d,p):PM6)	1.647	1.655	−13.7			
	ONIOM(CCSD/6-31G(d,p):PM6)	1.653	1.651	−13.0			
	ωB97X-D/6-31G(d,p)	1.579	1.593	−17.7	−52.9	−71.0	−140.1 (−130.5)
	M06-2X/6-31G(d,p)[c]	1.578	1.600	−15.9	−24.9	−42.3	−112.4 (−100.5)
	M06-2X/6-311 + G(d,p)//M06-2X/6-31G(d,p)[d]	1.679	1.686	−15.4	−24.9	−54.9	−119.9 (−100.1)
1.2$_4$.1_CC$_H$-1	ONIOM(M06-2X/6-31G(d,p):PM6)	1.562	1.628	−17.3			
	ONIOM(M06-2X/6-311 + G(d,p):PM6)	1.665	1.717	−16.5			
	M06-2X/6-31G(d,p)[c]	1.636	1.732	−16.8	−28.3	−45.9	−213.6 (−198.4)
	M06-2X/6-311 + G(d,p)//M06-2X/6-31G(d,p)[d]	1.708	1.790	−16.1	−28.3	−60.9	−230.6 (−197.3)
1.1_AC$_H$-1	ONIOM(M06-2X/6-31G(d,p):PM6)	1.906	1.551	−14.0			
	ONIOM(MP2/6-31G(d,p):PM6)	1.960	1.635	−10.5			
	ONIOM(CCSD/6-31G(d,p):PM6)	1.964	1.637	−9.7			
	ωB97X-D/6-31G(d,p)	2.637	1.623	−8.0	−54.8	−72.9	−142.2 (−132.6)
	M06-2X/6-31G(d,p)[c]	2.303	1.634	−9.5	−28.2	−44.6	−116.0 (−104.2)
1.2$_4$.1_AC$_H$-1	M06-2X/6-31G(d,p)[c]	1.940	1.653	−15.0	−31.3	−47.5	−215.0 (−199.8)
1.1_AA$_H$-1	ONIOM(M06-2X/6-31G(d,p):PM6)	1.830	1.927	−11.8			
	ONIOM(MP2/6-31G(d,p):PM6)	1.832	1.933	−9.1			
	ONIOM(CCSD/6-31G(d,p):PM6)	1.852	1.927	−8.5			
	ωB97X-D/6-31G(d,p)	2.934	3.017	−1.1	−55.5	−72.2	−142.4 (−132.8)
	M06-2X/6-31G(d,p)[c]	2.491	2.834	−0.5	−29.5	−44.5	−117.1 (−105.3)
1.2$_4$.1_AA$_H$-1	M06-2X/6-31G(d,p)[c]	1.933	2.008	−12.6	−34.0	−47.9	−215.3 (−200.1)

[a] BSSE-corrected values; $\Delta E = E$(dimer) − 2E(monomer) +BSSE; ΔE_1 = E(encapsulated complexes) − E(cage) − E(dimer) + $BSSE_1$; $\Delta E_2 = E$(encapsulated complexes) − E(cage) − 2E(monomer) + $BSSE_2$; $\Delta E_3 = E$(encapsulated complexes) − 2 E(**1**) − 2E(monomer) + $BSSE_3$ for the **1.1** cage and $\Delta E_3 = E$(encapsulated complexes) – 2E(1) – 4E(spacer) – 2E(monomer) + $BSSE_3$ for the **1.2$_4$.1** cage

[b] ΔE_3 energy with respect to the cavitands and spacers in the geometry of the capsule and in parenthesis with respect to the free geometry optimized cavitands and spacers

[c] Ref. [27]

[d] Ref. [28]

benzamide) cages has been calculated recently by our group at the M06-2X/6-31G(d,p) level of theory in order to rationalize the observed differences in the % distributions of the dimers formed [26, 27]. The results show that the % distribution of encapsulated dimers in the larger cage (for R = E) is similar to the gas-phase distribution [26]. In the smaller cage (for R = H), the interaction of amide with the cage leads to lower dimerization energy and a reduced % fraction of the corresponding encapsulated dimers, compared to the large cage % distribution [27], in agreement with experiment. We have shown that the very fast ONIOM methodology predicts similar results as the full DFT regarding the geometries of the lowest in energy encapsulated dimers and the % distribution of the dimers when the cavity of the cage is large enough, i.e., in **1.2$_4$.1** for R = E [26]. In the case of the compressed systems (R = M and E) in **1.1** [29], ONIOM(DFT:PM6) was found to be adequate for preliminary calculations given the great reduction in the required computational effort which is gained via the use of the PM6 methodology instead of full DFT methodology. It is in its favor that it predicts the same minimum energy structures as DFT methodologies, but it has the disadvantage that the energy ordering of the various structures of the encapsulated complexes is different from that of DFT.

In the case of encapsulation of heterodimers and homodimers of unsubstituted benzamide and benzoic acid in the **1.1** cage, the cavity has just enough space for the formation of dimers. It was previously found at the M06-2X/6-31G(d,p) methodology that an interaction of amide

Table 4 Dimer BSSE-corrected % distribution[a] of the $\mathbf{CC_R}$, $\mathbf{AC_R}$ and $\mathbf{AA_R}$ species free and encapsulated in **1.1**, $\mathbf{1.2_4.1}$ and **3.3** cages

	Methods	$\mathbf{CC_R}$	$\mathbf{AC_R}$	$\mathbf{AA_R}$
R = H				
Free	M06-2X/6-31G(d,p)[b]	27.7	50.7	21.6
	ωB97X-D/6-31G(d,p)	27.3	50.6	22.1
	MP2/6-31G(d,p)	26.8	50.8	22.4
	CCSD/6-31G(d,p)	27.0	50.8	22.1
In **1.1**	ONIOM(M06-2X/6-31G(d,p):PM6)	30–31	49–50	20–21
	ONIOM(MP2/6-31G(d,p):PM6)	30–31	48–50	20–21
	ONIOM(CCSD/6-31G(d,p):PM6)	30	50	20
	M06-2X/6-31G(d,p)[b]	47–57	35–38	5–18
	ωB97X-D/6-31G(d,p)	44–52	39–45	3–17
	Expt[c]	59[b]	22[b]	19[b]
In **3.3**	M06-2X/6-31G(d,p)	29	53	18
	Expt[c]	100[d]		
In $\mathbf{1.2_4.1}$	M06-2X/6-31G(d,p)[b]	28.2	50.5	21.3
R = Me				
Free	M06-2X/6-31G(d,p)	27.8	50.7	21.6
In $\mathbf{1.2_4.1}$	M06-2X/6-31G(d,p)	28.2	50.3	21.5
R = Ethe				
Free	M06-2X/6-31G(d,p)	27.7	50.7	21.6
In $\mathbf{1.2_4.1}$	M06-2X/6-31G(d,p)	28.4	50.3	21.3
	Expt[f]	36[d]	53[d]	11[d]

[a] The calculated gaps in % distribution result from the calculated ΔE dimerization values taking into account of the near-degenerated encapsulated structures and structures lying within 2 kcal/mol from the lowest minima

[b] Ref. [27]

[c] Experimental data, Ref. [25]

[d] Benzamide was not measurably encapsulated in 3.3 nor was the heterodimer **AC** in mesitylene-d12 solution

[e] Ref. [26]

[f] Experimental data, Ref. [23]

with the cage leads to lower dimerization energy and a reduced % fraction of the corresponding encapsulated dimers, compared to the free dimers % distribution, in agreement with experiment [27]. Thus, it is of interest to examine here whether the ONIOM(M06-2X:PM6) methodology can reproduce the findings of the M06-2X/6-31G(d,p) methodology [27]. In addition, ONIOM(MP2:PM6) and ONIOM(CCSD:PM6) methodologies are also examined. Furthermore, DFT calculations via another functional, i.e., ωB97X-D, have been carried out to check the agreement between the two functionals. The results are summarized in Tables 3 and 4 and in Tables 1S–2S of the supporting information (ESM).

The hydrogen bond distances between the monomers, dimerization energies of the encapsulated $\mathbf{A_H}$ and $\mathbf{C_H}$ guests inside the cage (ΔE), encapsulation energy of the dimers (ΔE_1), encapsulation energy of the monomers (ΔE_2) and formation energy of the encapsulated complexes with respect to the four components of fully disassembled complexes (ΔE_3) at various levels of theory are shown in Table 3. The % distribution of the dimers at various levels of theory is shown in Table 4.

We observe that the geometries, energy ordering and the dimerization energies of the encapsulated complexes which are predicted here via the ωB97X-D/6-31G(d,p) method are in agreement with the corresponding data of the M06-2X functionals [27], see Table 3 and Tables 1S–2S of the ESM. We have to note that the only difference between the two functionals is that the ωB97X-D ΔE_1, ΔE_2, ΔE_3 values are larger by the same amount ($\sim$28 kcal/mol) than the corresponding M06-2X values as in the case of the compressed systems due to the fact that the ωB97X-D functional includes long range and empirical dispersion corrections in calculations of interactions between the guests and the cavitands given that many long-range interactions can be observed between the cavitands and the guests and it is expected that the ωB97X-D functional will predict larger ΔE_1, ΔE_2, ΔE_3 interaction energies than M06-2X, see above.

Scheme 1 .

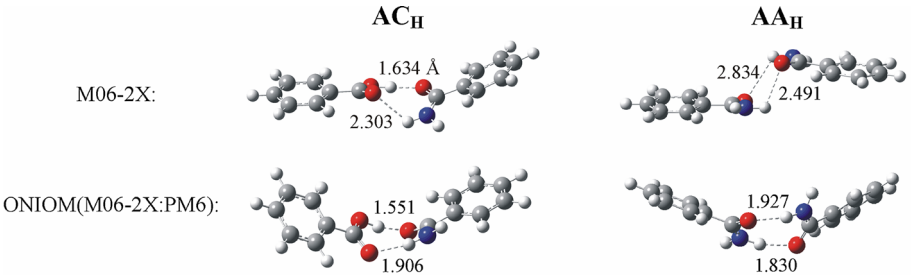

Scheme 2 .

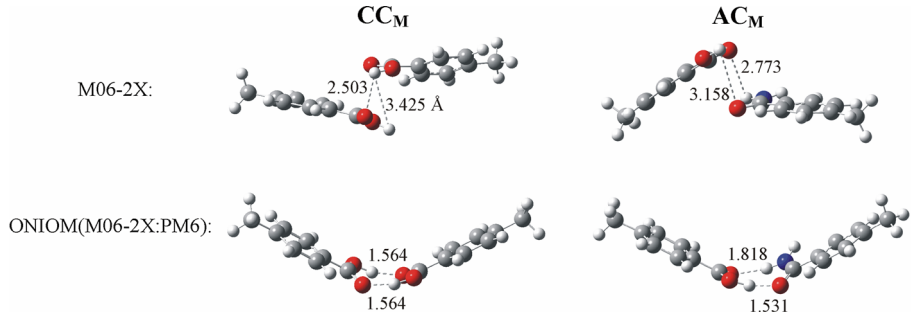

The present calculations via the ωB97X-D functional predict, as the M06-2X/6-31G(d,p) calculations [27], interaction only of the benzamide monomer in the homodimer or heterodimer with the cage. As a result, the pseudo ring formed by the two hydrogen bonds, for the $\mathbf{AA_H}$ and $\mathbf{AC_H}$, is not flat as in the case of the free dimers, see Fig. 2, but the two monomers are placed in different planes due to the interaction of the $\mathbf{A_H}$ with the cage, see Fig. 4. Thus, the NH…O hydrogen bonds are elongated compared to the free $\mathbf{AA_H}$ and $\mathbf{AC_H}$ dimers, see Tables 1 and 3 and Scheme 1. However, the ONIOM methodologies, i.e., ONIOM(M06-2X:PM6), ONIOM(MP2:PM6) and ONIOM(CCSD:PM6) where the dimers are calculated via DFT, MP2 or CCSD methods, predict that the two monomers forming the dimer are planes at an angle, see Fig. 4, with NH…O hydrogen bond similar to the corresponding distances of the free $\mathbf{AA_H}$ and $\mathbf{AC_H}$ dimers, see Scheme 1 where the encapsulated dimers $\mathbf{AA_H}$ and $\mathbf{AC_H}$ in **1.1** are shown (omitting the cage for clarity) in the lowest in energy minima for full DFT methodologies and ONIOM methodology.

Structures having the monomers placed in different planes are not stable via ONIOM methodologies, and they are converted into the presented minima of Fig. 4. Those encapsulated structures are low lying in energy for the full DFT methodologies, but they are not the lowest ones, see Fig. 4 and Tables 1S–2S and Figs. 1S and 3S of the ESM. This difference in the energy ordering of the minima between the ONIOM and the DFT methodologies is reflected also in the determination of the % distribution of the dimers. While, the full DFT methodologies predict % distributions of $\mathbf{CC_H}$, $\mathbf{AC_H}$ and $\mathbf{CC_H}$ of 5–18 [3–17], 35–38[39–45] and 47–57[44–52] % at the M06-2X/6-31G(d,p)[ωB97X-D/6-31G(d,p)] level of theory respectively reproducing the trend of the experimental % distributions of 19, 22 and 59 %, respectively [25], see Table 4, the ONIOM % distribution in the **1.1** cage is about 30, 50, 20 %, respectively, that corresponds to the free dimers not to the encapsulated in **1.1** cage. Thus, the use of PM6 for the cage, when the cavity of the cage is limited for the dimers, leads to wrong % dimer distributions. Note that in the above cases, the calculated gaps in % distribution result from the calculated ΔE dimerization values taking into account of the near-degenerated encapsulated structures and structures lying within 2 kcal/mol from the lowest minima. In the case of methyl-substituted guests in **1.1**, when the cavity is tight enough, again there are some differences between full DFT(M06-2X and ωB97X-D) and ONIOM(DFT:PM6) methodologies. The DFT lowest in energy encapsulated $\mathbf{AC_M}$ and $\mathbf{CC_M}$ systems are about 10 kcal/mol above the lowest ONIOM(DFT:PM6) structures [29]. The isolated $\mathbf{AC_M}$ and $\mathbf{CC_M}$ systems in **1.1** via the two methodologies are shown in Scheme 2. The ONIOM(DFT:PM6) predicts the formation of dimers in the **1.1** cage contrary to full DFT methodology, which predicts that the encapsulation is still favorable but the monomers prefer to be by themselves in the host, in agreement with the fact that encapsulated methyl dimers have not been found experimentally. In the case of ethyl-substituted guests in **1.1**, when the cavity is very tight, the differences between full DFT and ONIOM(DFT:PM6) methodologies are minimized, see Fig. 4, and both predict

that monomers prefer to be by themselves in the host, in agreement with the fact that encapsulated ethyl dimers have not been found experimentally.

Finally, for the heterodimer and the homodimers $\mathbf{CC_R}$, $\mathbf{AC_R}$ and $\mathbf{AA_R}$ dimers, where R = H, M and E in the $\mathbf{1.2_4.1}$ cage, both full DFT methodologies and ONIOM(DFT:PM6) methodologies present the same data with respect to geometry, dimerization energies and % dimer distribution in agreement with available experimental data [23] see Tables 3, 4 and 3S of the ESM. All dimers present almost the same % dimer distribution, i.e., 28($\mathbf{CC_R}$), 51($\mathbf{AC_R}$) and 21($\mathbf{AA_R}$), totally different from the case of the **1.1** cage.

Thus, the use of PM6 for cages with large or very tight cavity leads to correct % dimer distributions, while for tight cages it is unreliable. This can be attributed to the fact that the PM6 predicts a longer free **1.1** cage by 0.2 Å while the encapsulated complexes are longer by ~0.4 Å via ONIOM(DFT:PM6) than full DFT methodology. This is important in tight cages because it affects the relative energy ordering of the encapsulated complexes, while in large or very tight cages it does not affect the data.

Encapsulated dimers in 3.3 cage

As mentioned in the Introduction, the **3.3** cage offers a similar-size cavity as the **1.1** cage, and the difference between the two cavities is found in small differences between the cavitands **1** and **3** (cf. Fig. 1). The calculations find that the **3.3** cage is more stable than the **1.1** cage [28]: The first one has a formation energy with respect to their cavitands, calculated at −144.4 (−113.6), while the second one has a half formation energy, i.e., −69.4 (−57.5) kcal/mol, with respect to the respective cavitands **3** or **1**, fixed in the geometry of the capsule and, in parentheses, with respect to the free optimized cavitands at the M06-2X/6-31G(d,p) level of theory, see Fig. 1.

Experimentally, it has been observed that co-encapsulation of benzoic acid and benzamide in the case of **1.1** leads to the formation of all three possible encapsulated dimers, $\mathbf{CC_H}$, $\mathbf{AC_H}$ and $\mathbf{AA_H}$, whereas in the case of **3.3** only encapsulated $\mathbf{CC_H}$ has been observed in mesitylene-d12 solution. Here we are investigating this problem by M06-2X/6-31G(d,p) calculations and geometry optimization to determine the possible minimum energy structures in an attempt to provide an explanation for the above experimental findings taking into account the experimental conditions.

The calculations find stable structures for all encapsulated dimers showing that all dimers can be encapsulated. The three lowest calculated minimum energy structures for each encapsulated $\mathbf{CC_H}$, $\mathbf{AC_H}$ and $\mathbf{AA_H}$ complexes in the **3.3** cage are depicted in Fig. 5. The hydrogen bond lengths between the encapsulated monomers and the monomers and the cavitands, the dimerization energies (ΔE), the encapsulation energies of dimers (ΔE_1) and of monomers (ΔE_2), the formation energies of the complexes (ΔE_3) and the relative energy ordering of the isomers are given in Table 5. The interaction energies range from −6 to −18 (ΔE), from −19 to −28 (ΔE_1), from −29 to −43 (ΔE_2) and from −164 to −186 kcal/mol (ΔE_3) at the M06-2X/6-31G(d,p) level of theory, see Table 5. For the lowest minima of each of the three dimers, the ΔE_1, ΔE_2 and ΔE_3 interaction energies are very similar.

In all isomers with the exception of the **3.3_AA$_H$-3** isomer, the guests form dimers. In all isomers, weak hydrogen bonds, i.e., hydrogen bonds with large bond lengths, are formed between the guests and the cavitands with bond distances that range from 2.4 to 3.2 Å. Conversely, the **3.3_AA$_H$-3** isomer is mainly stabilized by interactions with the walls of the capsule. In all free dimers three rings exist, i.e., the two phenyl rings and the ring that is formed by the two hydrogen bonds between the monomers cf. Fig. 2. In the case of the free **CC** dimer, the three rings lie in the same plane; in the free $\mathbf{AC_H}$ dimer, the $\mathbf{C_H}$ phenyl ring and the ring that is formed between the two monomers lie in the same plane, while in the free $\mathbf{AA_H}$ dimer, the two phenyl rings lie in the same plane, see Fig. 2. The hydrogen bond lengths OH…O and NH…O of the dimers range from 1.54 to 1.66 Å and 1.80 to 1.97 Å, respectively, for all encapsulated complexes except from **3.3_AA$_H$-3**. The corresponding values of the free monomers are 1.558 Å for the **CC** dimer, 1.578 and 1.844 Å for the **AC** dimer and 1.855 Å for the $\mathbf{AA_H}$ dimer. Note that the **3.3_CC$_H$-3**, **3.3_AC$_H$-3** and **3.3_AA$_H$-2** have slightly decreased hydrogen bond length compared to the free dimers due to the slight compression of the cage. The fact that the slight compression results in a decrease in the hydrogen bond length has been found experimentally in the case of encapsulation on different carboxylic acid dimers in the **1.1** cage [24]. Finally, we should note that the second hydrogen atom of the amide group forms hydrogen bonds with the walls of the cage having bond lengths of 2.3–2.8 Å. As a result a small additional stabilization of the structures is obtained.

In the encapsulated dimers, only in the **3.3_CC$_H$-3** complex the dimer is almost the same as the free one and as a result its dimerization energy 17.7 kcal/mol, the same with the free one, i.e., 17.8 kcal/mol, see Table 5 and Fig. 2. In the **3.3_CC$_H$-1**, **3.3_AC$_H$-1** and **3.3_AC$_H$-3** complexes, the two monomers form a small angle of about 14 degrees and their dimerization energy is reduced by about 1 kcal/mol compared to the free ones, i.e., their ΔE are −16.5, −15.2 and −15.0 kcal/mol, while the corresponding values of the free dimers are −17.8 ($\mathbf{CC_H}$) and −16.3 ($\mathbf{AC_H}$) kcal/mol. In the **3.3_CC$_H$-2** and **3.3_AC$_H$-2**, the two monomers form a very small angle and their dimerization energy is reduced by about 0.5 kcal/mol compared to the free ones, i.e., their ΔE are −17.3 and

Table 5 Hydrogen bond distances (R in Å), dimerization energies of the encapsulated $\mathbf{A_H}$ and $\mathbf{C_H}$ guests inside the cage (ΔE, in kcal/mol)[a], encapsulation energy of the dimers (ΔE_1 in kcal/mol)[a], encapsulation energy of the monomers (ΔE_2 in kcal/mol)[a] and formation energy of the encapsulated complexes with respect to the four components of fully disassembled complexes (ΔE_3 in kcal/mol),[a] and the relative energy ordering (T_e in kcal/mol) of the isomers of the **3.3_CC$_H$**, **3.3_AC$_H$** and **3.3_AA$_H$** encapsulated complexes at the M06-2X/6-31G(d,p) level of theory

Species	R_{3-4}[b]	R_{7-8}[b]	$R_{H...O}$[c]	$R_{H...O}$[c]	$R_{O...Hc}$[d]	$R_{O...Hc}$[e]	$R_{H...Oc}$[d]	$R_{O...Hc}$[e]	ΔE[f]	ΔE_1[g]	ΔE_2[h]	ΔE_3[i]	T_e[j]
3.3_CC$_H$-1	1.650	1.659			2.806	2.928	2.609	2.982	−16.5	−24.8	−42.5	−186.1 (155.3)	0.0 (0.0)
3.3_CC$_H$-2	1.546	1.571			2.912	3.036	2.844	2.975	−17.3	−19.3	−36.8	−180.2 (149.4)	1.6 (6.0)
3.3_CC$_H$-3	1.539	1.555			2.849	3.066	3.041	3.174	−17.7	−17.8	−35.2	−178.5 (147.7)	2.2 (7.6)
3.3_AC$_H$-1	1.897	1.564	2.490		2.898	2.740	2.765	2.983	−15.2	−26.7	−42.7	−186.3 (155.5)	0.0 (0.0)
3.3_AC$_H$-2	1.861	1.548	2.605		2.728	3.037	2.819	3.094	−15.7	−20.1	−36.1	−179.5 (148.7)	2.9 (6.8)
3.3_AC$_H$-3	1.801	1.558	2.837		2.970	2.751	2.765	3.031	−15.0	−12.6	−28.5	−164.0 (133.2)	10.2 (22.3)
3.3_AA$_H$-1	1.786	1.974	2.423	2.422	2.837	2.799	2.786	2.594	−10.7	−27.5	−41.2	−184.9 (154.1)	0.0 (0.0)
3.3_AA$_H$-2	1.852	1.853	2.353	2.356	2.909	2.765	2.908	2.763	−11.8	−18.9	−32.6	−176.2 (145.4)	3.8 (8.7)
3.3_AA$_H$-3	3.832	3.121	2.322	2.387	2.446	2.642	2.663	2.941	−5.8	−21.7	−35.8	−178.9 (148.1)	5.3 (6.0)

[a] BSSE-corrected values

[b] Hydrogen bond distance between the two monomers

[c] The hydrogen bond distance between second hydrogen atom of the amide group and oxygen atom of the cage

[d] The shortest hydrogen bond distance between hydrogen atom of the monomers and oxygen atom of the cage

[e] The shortest hydrogen bond distance between oxygen atom of the monomers and hydrogen atom of the cage

[f] $\Delta E = -[E(\text{dimer}) - 2E(\text{monomer})]$

[g] $\Delta E_1 = -[E(\text{encapsulated complexes}) - E(\text{cage}) - E(\text{dimer})]$

[h] $\Delta E_2 = -[E(\text{encapsulated complexes}) - E(\text{cage}) - 2E(\text{monomer})]$

[i] $\Delta E_3 = -[E(\text{encapsulated complexes}) - 2\,E(\mathbf{1}) - 2E(\text{monomer})]$; ΔE_3 energy with respect to the cavitands and spacers in the geometry of the capsule and in parenthesis with respect to the geometry optimized free cavitands and spacers

[j] Relative energy ordering without BSSE (with respect to BSSE)

−15.7 kcal/mol. Finally, the **3.3_AA$_H$-1** and **3.3_AA$_H$-2** dimer complexes have the two monomers at an angle of about 140 degrees, while the **3.3_AA$_H$-3** complex has one monomer lying above the other, see Fig. 5. As a result of the above distortion compared to the free $\mathbf{AC_H}$ dimer, their dimerization energies are reduced to −10.7, −11.8 and −5.8 kcal/mol, respectively, compared to the −13.9 kcal/mol of the free $\mathbf{AC_H}$ dimer. So, the encapsulated $\mathbf{CC_H}$ dimer is slightly distorted, $\mathbf{AC_H}$ is more distorted, while $\mathbf{AA_H}$ is the most distorted dimer. A theoretical distribution of 29 % (**3.3_CC$_H$**), 53 % (**3.3_AC$_H$**) and 18 % (**3.3_AA$_H$**) is obtained using the dimerization energy of the lowest in energy complexes or the average values of three encapsulated dimers (**3.3_CC$_H$**), 1 (**3.3_AC$_H$**) and 1 (**3.3_AA$_H$**), i.e., the energy difference between encapsulated complexes is within 2 kcal/mol, see Table 4. This distribution is based on the capability of encapsulation of the three dimers irrespectively to the other conditions in the solution. However, while the approach employed for the determination of the % dimer distribution works quite well and explains the experimental funding in the case of the free and encapsulated $\mathbf{CC_R}$, $\mathbf{AC_R}$, $\mathbf{AA_R}$, R = H, M and E in the **1.1** and **1.2$_4$.1** cages, see above, it does not reproduce the experimental findings for the **3.3** cage. The explanation to this fact results from the differences between **1.1** (or **1.2$_4$.1**) and **3.3** and the conditions in the solution which should be taken into account.

The **1.1** and **3.3** cages have the same length of 17.5 Å, see Fig. 1, but they differ at the sixteen N–H…O hydrogen bond distances between the two cavitands in both cages. In **3.3** the bond lengths are about 1.89 Å similar to the N–H…O hydrogen bonds of 1.86 Å, when there are no structural constraints [37], while in **1.1** the hydrogen bonds are elongated by 0.25 Å, i.e., ∼2.12 Å. As a result, the formation energy with respect to the free optimized cavitands is for **3.3** twice than the corresponding value for **1.1**, i.e., −57.5 kcal/mol for **1.1** and −113.6 kcal/mol for **3.3**. The average interaction energy of N–H…O hydrogen bond is 3.6 kcal/mol in **1.1** and 7.1 kcal/mol in **3.3**. This value is similar to the interaction energy of 7.3 kcal/mol for the N–H…O hydrogen bonds of 1.86 Å, when there are no structural constraints [37]. In the extended capsule assembly **1.2$_4$.1** (with a central axis length of 23.7 Å), thirty-two N–H…O hydrogen bonds are formed, the bond lengths between the cavitands and the spacers range from 1.65 to 2.57 Å, while the bond length between the spacers is about 1.97 Å. Note that the formation energy for the **1.2$_4$.1** cage is calculated at −154.5 kcal/mol with respect to the free optimized cavitands and four spacers and the

Table 6 Average encapsulation energy[a] (kcal/mol) of the $\mathbf{CC_R}$, $\mathbf{AC_R}$ and $\mathbf{AA_R}$ dimers in **1.1**, $\mathbf{1.2_4.1}$ and **3.3** cages at the M06-2X/6-31G(d,p)

	$\mathbf{CC_H}$	$\mathbf{AC_H}$	$\mathbf{AA_H}$	$\mathbf{CC_M}$	$\mathbf{AC_M}$	$\mathbf{AA_M}$	$\mathbf{CC_E}$	$\mathbf{AC_E}$	$\mathbf{AA_E}$
1.1	−23.5	−27.2	−30.5	−10.6	−14.9	−22.9	−11.7	−12.5	−23.8
$\mathbf{1.2_4.1}$	−28.3	−31.3	−34.0	−33.6	−36.7	−36.6	−38.7	−40.8	−41.7
3.3	−20.6	−23.4	−23.2						

[a] Corrected values for BSSE; average values taking into account of the near-degenerated encapsulated structures and structures lying within 2 kcal/mol from the lowest minima

average interaction energy of the N–H…O hydrogen bonds is 4.8 kcal/mol. Thus, the **1.1** and $\mathbf{1.2_4.1}$ cages open more easily or at least partly open than **3.3**. Additionally, the encapsulation energy of the $\mathbf{AA_H}$ and $\mathbf{AC_H}$ dimers is significantly larger by about 30 % in **1.1** and $\mathbf{1.2_4.1}$ than in **3.3**, see Table 6. This factor in conjunction with the fact that primary amides tend to form hydrogen-bonded network in solution [43] results in the conclusion that the smaller encapsulation energy in **3.3** can act competitively to energy gain from the hydrogen network of primary amide, see Fig. 4S of ESM.

The lowest in energy minimum structures of hydrogen-bonded network of benzamide formed by three to six benzamide molecules are depicted in Fig. 6. In the calculated structures, four to ten hydrogen bonds are formed. The formation energies of the networks are given in Fig. 6. In the cases of the clusters of four and six benzamide molecules, two minima were calculated forming a different type of hydrogen-bonded network. The energy hydrogen bond interactions of the calculated structures range from 24.7 to 71.1 kcal/mol (see Fig. 6), their average interaction per hydrogen bond ranges from 6.2($\mathbf{A_3}$) to 7.1($\mathbf{A_6}$-**1**) kcal/mol, while the hydrogen bond distances range from 1.724 to 2.088 Å. Thus, in the cases of the **1.1** and $\mathbf{1.2_4.1}$ cages, energetically the encapsulation is not preferred when the average hydrogen-bonded networks of benzamide that are formed have six or more hydrogen bonds per cage, while in **3.3** when the average hydrogen-bonded networks of benzamide have less hydrogen bonds per cage, i.e., four hydrogen bonds. Some hydrogen-bonded networks of benzamide are shown in Fig. 4S of ESM. It should be noted that in solution, there are $\mathbf{CC_H}$, $\mathbf{AC_H}$ and $\mathbf{AA_H}$ dimers and $\mathbf{A_H}$ hydrogen-bonded networks in a dynamic equilibrium. All dimers and $\mathbf{A_H}$ network change partners.

Summarizing, the theoretical calculations predict the existence of encapsulated dimers in the **3.3** cage, whereas the **AA** homodimer and the **AC** heterodimer were not detected in the **3.3** experimentally via NMR spectra, in mesitylene-d12 solution [25]. The absence of observation of any **3.3**_$\mathbf{AC_H}$ and **3.3**_$\mathbf{AA_H}$ dimers is attributed here to two factors: one factor has to do with the greater stability of the **3.3** cage compared to **1.1** (where all three encapsulated dimers have been observed), making the opening and closing of the **3.3** cage energetically less favorable, and the second factor is the larger encapsulation energy of the $\mathbf{AC_H}$ and $\mathbf{AA_H}$ dimers obtained in **1.1** (and $\mathbf{1.2_4.1}$) than in **3.3** in combination with the tendency of benzamide to form hydrogen network. Smaller hydrogen networks act more antagonistically to encapsulation of the $\mathbf{AC_H}$ and $\mathbf{AA_H}$ dimers in **3.3** than in **1.1** (and $\mathbf{1.2_4.1}$).

Comparisons and trends in encapsulated dimers in 1.1, $\mathbf{1.2_4.1}$ and 3.3 cages

Here results of previous and present calculations are combined to determine trends in quantities relevant to encapsulated complexes. The dimerization energies of the heterodimers and homodimers of the substituted benzamide and benzoic acid with respect to the R are depicted in Fig. 7. In general, in all cases we observe similar trends for all computational methods employed. We see that all encapsulated dimers in $\mathbf{1.2_4.1}$ cage, for all three R groups (H, methyl, ethyl), have similar dimerization energies as the free dimers. They are smaller by 1.0–2.5 kcal/mol than the free dimers, see Fig. 7 and Tables 1 and 3. The size of the dimerization energies is similar in the free and encapsulated dimers in $\mathbf{1.2_4.1}$ cage and as a result the % distribution of the dimers is the same, see Tables 1 and 4. In the case of the encapsulated dimers in the **1.1** cage, we observe that for the $\mathbf{CC_R}$ dimer, the dimerization energies are similar to the free $\mathbf{CC_R}$ dimers for R = H, but for R = M the dimerization energies are very small or the dimer does not exist (for full DFT methods) showing that in the cage exist two non-interacting encapsulated monomers and the monomers prefer to be by themselves in the host. However, as the R increased to ethyl group, the monomers are forced to be close enough due to the small cavity, and we observe an increase in the dimerization energy due to π-stacking, with respect to the R = M, even though the usual hydrogen-bonded dimers do not form. In the case of the encapsulated $\mathbf{AA_R}$ and $\mathbf{AC_R}$ dimers in the **1.1** cage, we observe that for R = H very small ΔE values for $\mathbf{AA_R}$ and half of the ΔE values of the free dimers for $\mathbf{AC_R}$ are obtained. However, as the R increase to R = E the dimerization energy decreases significantly and the dimers are not formed, but there are two monomers in the cavity, see Fig. 7 and Tables 1 and 3.

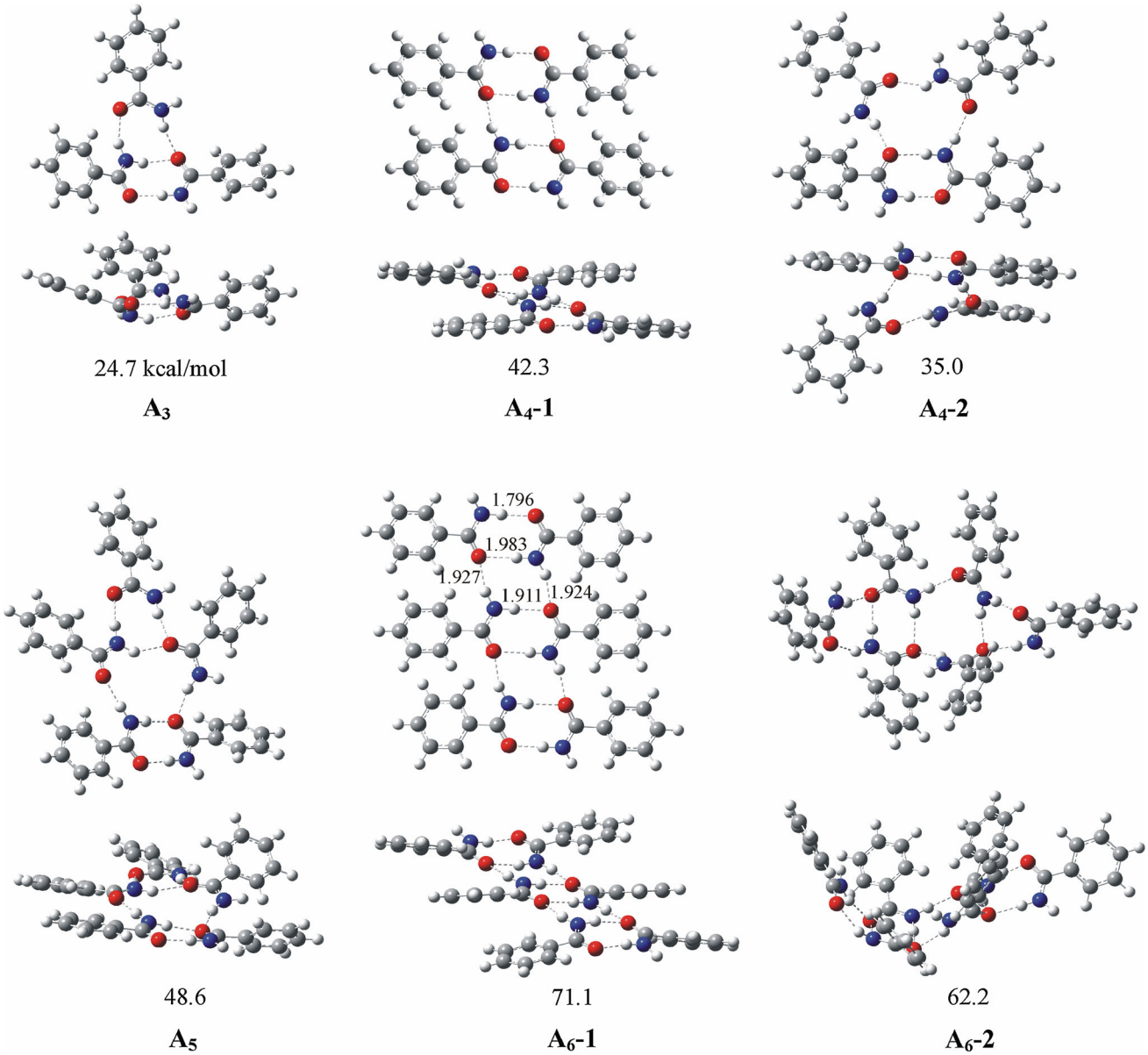

Fig. 6 Calculated structures of the lowest minima of three to six benzamide molecules viewed from two different angles (Color online; H atoms = *white spheres*, C = *gray spheres*, O = *red spheres* and N = *blue spheres*). The formation energies of the structures are given at the M06-2X/6-31G(d,p) level of theory

The encapsulation energies of the dimers (ΔE_1), of the monomers (ΔE_2) and the formation energy of the complexes with respect to the four or eight components of fully disassembled complexes (ΔE_3) of substituted benzamide and benzoic acid with respect to the R group at various levels of theory are depicted in Figs. 8, 9, 10. In general, all the ΔE_1, ΔE_2 and ΔE_3 energies are reduced as the R size is increased for the **1.1** cage and increased for the **1.2$_4$.1** cage. The DFT methodologies present the same trends with the only difference that the ωB97X-D values are larger by the same amount, see above. The ONIOM(M06-2X/6-311 + G(d,p):M06-2X/6-31G(d,p)) methodology [28] presents the same values with the M06-2X/6-31G(d,p) method for the ΔE_1 and ΔE_3 energies, but it computes increased values for the ΔE_2 energies by about 15 kcal/mol.

The OH…O and NH…O hydrogen bond distances of the **CC$_R$**, **AC$_R$** and **AA$_R$** encapsulated dimers with respect to the R group at various levels of theory are depicted in Figs. 5S and 6S of the ESM. We observe that the hydrogen bond distances of the dimers in the **1.2$_4$.1** cage remain the same as the R size increased for all methods, while in the **1.1** cage are increased as the R became the ethyl group in all methods. In other words, the ONIOM seems that do not

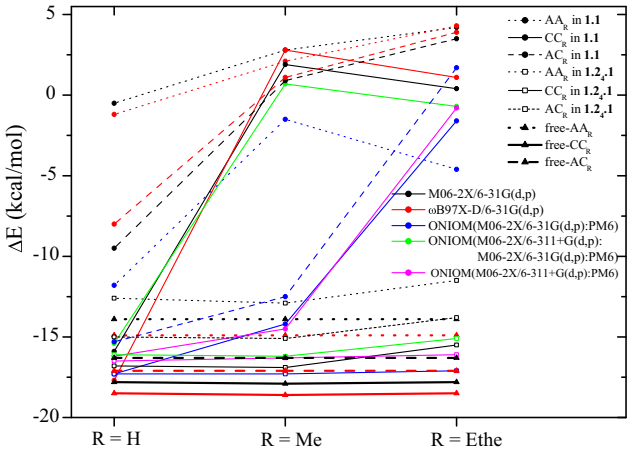

Fig. 7 Dimerization energies of the dimers of substituted benzamide and benzoic acid with respect to the R group at various levels of theory

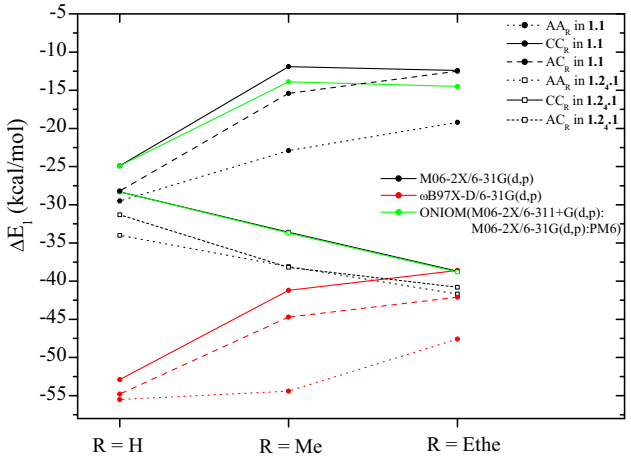

Fig. 8 Encapsulation energy of the dimers (ΔE_1) of substituted benzamide and benzoic acid with respect to the R group at various levels of theory

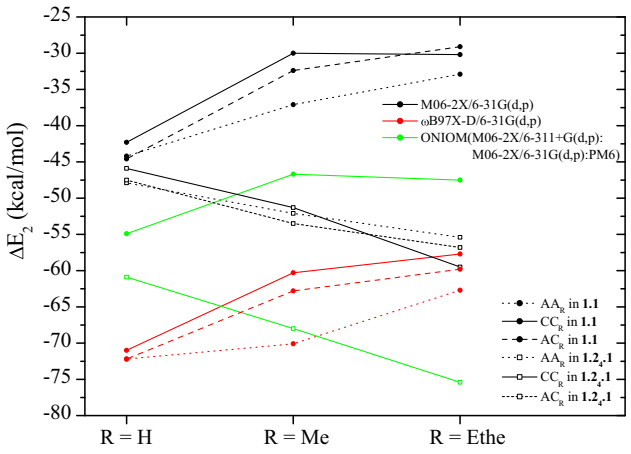

Fig. 9 Encapsulation energy of the dimers (ΔE_2) of substituted benzamide and benzoic acid with respect to the R group at various levels of theory

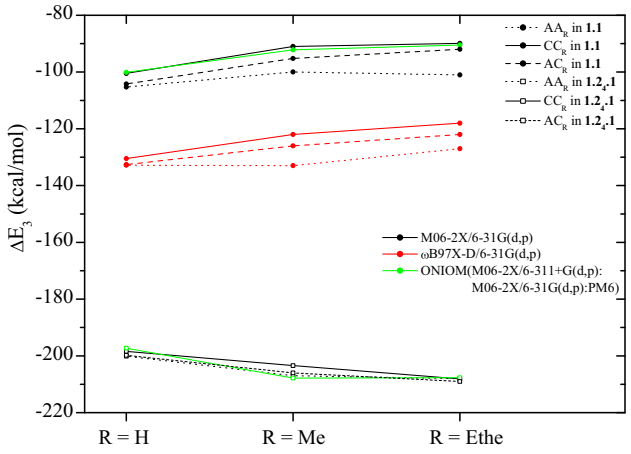

Fig. 10 Formation energy of the encapsulated complexes with respect to the four or eight components of fully disassembled complexes (ΔE_3) of substituted benzamide and benzoic acid with respect to the R group at various levels of theory

predict well the NH…O hydrogen bond distances for the unsubstituted and methyl-substituted guests and OH…O hydrogen bond distances for the methyl-substituted guests in **1.1** because the dimers are retained in ONIOM.

As noted previously, the **1.1** and **3.3** cages have almost the same cavity's size, see Fig. 1, but the formation energy of **3.3** is twice than the corresponding value of the **1.1** cage. As a result for the encapsulation of the $\mathbf{CC_H}$ dimer, the ΔE, ΔE_1 and ΔE_2 values are similar for the two cages, but the ΔE_3 values are significant larger in **3.3** than in **1.1**. In **3.3** only the $\mathbf{CC_H}$ was detected experimentally contrary to what happen in **1.1** and $\mathbf{1.2_4.1}$ cages [25], as explained before.

The encapsulation energy of the dimers in the $\mathbf{1.2_4.1}$ cage is increased as R increased, while in the **1.1** cage the value is decreased when R = H become substituted by methyl of ethyl group, see Table 6. In **3.3** the encapsulations energies are smaller than in **1.1** and $\mathbf{1.2_4.1}$ for all dimers, and as mentioned before, the smaller encapsulation energies lead to act the encapsulation of $\mathbf{AA_H}$ and $\mathbf{AC_H}$ competitively to smaller hydrogen-bonded networks.

Conclusions

Encapsulation complexes are tools of physical organic chemistry on the nanoscale since organic cages are capable of molecular recognition, isolation of reactive species and promoting reactions [44–46]. In the present study via theoretical calculations, we study the encapsulation of single monomers, homodimers and heterodimers of benzoic acid and benzamide and their methyl- and ethyl-substituted dimers in three cages as well as hydrogen-bonded networks

of benzamide having three to six molecules. The trends of the encapsulation with respect to the hydrogen bond distance, dimerization energy, % dimer distribution, encapsulation energies and formation energies, as the size of the dimers is increased are presented. All three types, unsubstituted and methyl- and ethyl-substituted encapsulated dimers, present the same % dimer distribution with the free dimers in agreement with any available experimental data in the large cage (**1.2$_4$.1**). In the small **1.1** cage, the % dimer distribution for the unsubstituted dimers is totally different from that in the large cage, and as the size of the dimers increased, the dimers are not longer exist but exist as co-encapsulated monomers.

The % encapsulated dimer distribution in **3.3** and **1.1** cages which have the same size differs substantially. Theoretical calculations predict the existence of encapsulated dimers in the **3.3** cage, where the $\mathbf{AA_H}$ homodimer and the $\mathbf{AC_H}$ heterodimer are distorted with respect to the free dimers. However, the $\mathbf{AA_H}$ and $\mathbf{AC_H}$ dimers were not detected in the **3.3** experimentally via NMR spectra, in mesitylene-d12 solution [25]. Their absence of observation is attributed here mainly to two factors: one factor has to do with the greater stability of the **3.3** cage compared to **1.1** (where all three encapsulated dimers have been observed), making the opening and closing of the **3.3** cage energetically less favorable and the second factor is the fact that primary amides tend to form networks in solution. In addition, smaller encapsulation energies are observed in **3.3** compared to other two cages. The smaller energy gained in **3.3** for the encapsulation of the $\mathbf{AA_R}$ and $\mathbf{AC_R}$ dimers can act competitively to energy gain from a smaller hydrogen-bonded network of primary amide than in **1.1** (or **1.2$_4$.1**).

Regarding the efficacy of ONIOM(DFT:PM6) methodology which has many successful applications [47–50], we found that for the encapsulation of the dimers in the cage with a large cavity or a very tight cavity, ONIOM(DFT:PM6) is in agreement with full DFT calculations and experimental data. However, when the cavity is enough tight, ONIOM(DFT:PM6) and ONIOM(MP2 or CCSD:PM6) methodologies fail. They are in disagreement with the experimental data, while full DFT calculations are in agreement. This is attributed to the fact that PM6 predicts slight longer cavity than DFT does and this is important in tight cages, because it affects the relative energy ordering of the encapsulated complexes, while in large or very tight cages the elongation does not affect the data. In general, it is not practical or feasible, and sometimes meaningless, to use high-level quantum chemistry to treat all atoms in a large complex [46]; thus, with caution the use of the ONIOM using PM6 for the low layer can provide good results.

Acknowledgments

Funding Financial support from GSRT and the EC through the European Fund for Regional Development, NSRF 2007–2013 action Development of Research Centers—KRHPIS, Project "New Multifunctional Nanostructured Materials and Devices—POLYNANO" to DT, IDT and GT is acknowledged.

Compliance with ethical standards

Conflict of interest The authors declare that they have no conflict of interest.

References

1. Lehn J-M (1995) Supramolecular chemistry: concepts and perspectives. VCH, Weinheim
2. Steed JW, Atwood JL (2000) Supramolecular chemistry. Wiley, New York
3. Beer PD, Gale PA, Smith DK (1999) Supramolecular chemistry. Oxford University Press, Oxford
4. Sherman JC, Jasat A (1999) Chem Rev 99:931–967
5. Cram DJ, Cram JM (1994) Container molecules and their guests. The Royal Society of Chemistry, Cambridge
6. Branda N, Grotzfeld RM, Valdés C, Rebek J Jr (1995) J Am Chem Soc 117:85–88
7. de Mendoza J (1998) Chem Eur J 4:1373–1377
8. Prins LJ, Reinhoudt DN, Timmerman P (2001) Angew Chem Int Ed 40:2382–2426
9. Conn MM, Rebek J Jr (1997) Chem Rev 97:1647–1668
10. Corbellini F, Fiammengo R, Timmerman P, Crego-Calama M, Versluis K, Heck AJR, Luyten I, Reinhoudt DN (2002) J Am Chem Soc 124:6569–6575
11. Ajami D, Liua L, Rebek J Jr (2015) Chem Soc Rev 44:490–499
12. Turner DR, Pastor A, Alajarin M, Steed JW (2004) Supramolecular assembly via hydrogen bonds I: book series. Struct Bond 108:97–168
13. Grawe T, Schrader T, Gurrath M, Kraft A, Osterod F (2000) J Phys Org Chem 13:670–673
14. Grawe T, Schrader T, Zadmard R, Kraft A (2002) J Org Chem 67:3755–3763
15. Fiedler D, Leung DH, Bergman RG, Raymond KN (2005) Acc Chem Res 38:349–358
16. Fujita M, Umemoto K, Yoshizawa M, Fujita N, Kusukawa T, Biradha K (2001) Chem Comm 509–518
17. Xantheas SS ed (2000) Recent theoretical and experimental advances in hydrogen bonded clusters. Kluwer Academic Publishers, NATO ASI Series C: Mathematical and Physical Sciences, p 561
18. Desiraju GR, Steiner T (1999) The weak hydrogen bond in structural chemistry and biology. Oxford University Press, New York
19. Gora RW, Grabowski SJ, Leszczynski J (2005) J Phys Chem A 109:6397–6405
20. Pašalić H, Aquino AJA, Tunega D, Haberhauer G, Gerzabek MH, Georg HC, Moraes TF, Coutinho K, Canuto S, Lischka H (2010) Comput Chem 31:2046–2055
21. Lucas B, Grégoire G, Lecomte F, Reimann B, Schermann JP, Desfrançois C (2005) Mol Phys 103:1497–1503
22. Daly AM, Sargus BA, Kukolich SG (2010) J Chem Phys 133:174304

23. Ajami D, Dube H, Rebek J Jr (2011) J Am Chem Soc 133:9689–9691
24. Ajami D, Tolstoy PM, Dube H, Odermatt S, Koeppe B, Guo J, Limback HH, Rebek J Jr (2011) Angew Chem Int Ed 50:528–531
25. Jiang W, Tiefenbacher K, Ajami D, Rebek J Jr (2012) Chem Sci 3:3022–3025
26. Tzeli D, Theodorakopoulos G, Petsalakis ID, Ajami D, Rebek J Jr (2011) J Am Chem Soc 133:16977–16985
27. Tzeli D, Petsalakis ID, Theodorakopoulos G, Ajami DW, Jiang Rebek J Jr (2012) Chem Phys Lett 548:55–59
28. Tzeli D, Petsalakis ID, Theodorakopoulos G (2013) Chem Phys Lett 573:48–55
29. Tzeli D, Petsalakis ID, Theodorakopoulos G, Ajami D, Rebek J Jr (2014) Theor Chem Acc 133:1503–1508
30. Zhao Y, Truhlar DG (2008) Theor Chem Acc 120:215–241
31. Zhao Y, Truhlar DG (2008) Acc Chem Res 41:157–167
32. Chai JD, Head-Gordon M (2008) Phys Chem Chem Phys 10:6615–6620
33. Curtiss LA, McGrath MP, Blaudeau JP, Davis NE, Binning RC Jr, Radom L (1995) J Chem Phys 103:6104–6113
34. Dapprich S, Komáromi I, Byun KS, Morokuma K, Frisch MJ (1999) J Mol Struct (Theochem) 462:1–21
35. Vreven T, Morokuma K, Farkas Ö, Schlegel HB, Frisch MJ (2003) J Comp Chem 24:760–769
36. Vreven T, Morokuma K (2006) Annu Rep Comp Chem 2:35–50
37. Tzeli D, Theodorakopoulos G, Petsalakis ID, Ajami D, Rebek J Jr (2013) Int J Quantum Chem 113:734–739
38. Heinz T, Rudkevich DM, Rebek J Jr (1998) Nature 394:764–766
39. Choi HJ, Park YS, Cho CS, Koh K, Kim SH, Paek K (2004) Org Lett 6:4431–4433
40. Boys SF, Bernardi F (1970) Mol Phys 19:553–566
41. Xantheas SS (1994) J Chem Phys 104:8821–8824
42. Gaussian 09, Revision A.1, Frisch MJ, Trucks GW, Schlegel HB, Scuseria GE, Robb MA, Cheeseman JR, Scalmani G, Barone V, Mennucci B, Petersson GA, Nakatsuji H, Caricato M, Li X, Hratchian HP, Izmaylov AF, Bloino J, Zheng G, Sonnenberg JL, Hada M, Ehara M, Toyota K, Fukuda R, Hasegawa J, Ishida M, Nakajima T, Honda Y, Kitao O, Nakai H, Vreven T, Montgomery Jr JA, Peralta JE, Ogliaro F, Bearpark M, Heyd JJ, Brothers E, Kudin KN, Staroverov VN, Kobayashi R, Normand J, Raghavachari K, Rendell A, Burant JC, Iyengar SS, Tomasi J, Cossi M, Rega N, Millam NJ, Klene M, Knox JE, Cross JB, Bakken V, Adamo C, Jaramillo J, Gomperts R, Stratmann RE, Yazyev O, Austin AJ, Cammi R, Pomelli C, Ochterski JW, Martin RL, Morokuma K, Zakrzewski VG, Voth GA, Salvador P, Dannenberg JJ, Dapprich S, Daniels AD, Farkas Ö, Foresman J B, Ortiz JV, Cioslowski J, Fox DJ (2009) Gaussian, Inc., Wallingford
43. Seo M, Park J, Kim SY (2012) Org Biomol Chem 10:5332–5342
44. Mitra T, Jelfs KE, Schmidtmann M, Ahmed A, Chong SY, Adams DJ, Cooper AI (2013) Nature Chem 5:276–281
45. Hof F, Craig SL, Nuckolls C, Rebek J Jr (2002) Angew Chem Int Ed 41:1488–1508
46. Zerkoune L, Angelova A, Lesieur S (2014) Nanomaterials 4:741–765
47. Chung LW, Sameera WMC, Ramozzi R, Page AJ, Hatanaka M, Petrova GP, Harris TV, Li X, Ke Z, Liu F, Li HB, Ding L, Morokuma K (2015) Chem Rev 115:5678–5796
48. Tzeli D, Petsalakis ID, Rebek T Jr (2015) J Chem Phys Lett 633:99–104
49. Tzeli D, Theodorakopoulos G, Petsalakis ID, Ajami D, Rebek J Jr (2012) J Am Chem Soc 134:4346–4354
50. Cantillo D, Ávalos M, Babiano R, Cintas P, Jiménez JL, Palacios JC (2011) Org Biomol Chem 9:7638–7642